

Synthesis, characterisation and thermal behaviour of solid state compounds of 4-methylbenzylidenepyruvate with some bivalent metal ions

I.A. Petroni, F.L. Fertoni, C.B. Melios, M. Ionashiro*

Instituto de Química, UNESP, C.P. 355, CEP 14801-970, Araraquara, SP, Brazil

Received 5 June 2002; received in revised form 26 September 2002; accepted 29 September 2002

Abstract

Solid state M-4-Me-BP compounds, where M stands for bivalent Mn, Fe, Co, Ni, Cu, Zn, Pb and 4-Me-BP is 4-methylbenzylidenepyruvate, have been synthesized. Simultaneous thermogravimetry-differential thermal analysis (TG-DTA), differential scanning calorimetry (DSC), X-ray powder diffractometry, infrared spectroscopy, elemental analysis, and complexometry were used to characterise and to study the thermal behaviour of these compounds. The results led to information about the composition, dehydration, thermal stability and thermal decomposition of the isolated complexes.

© 2002 Elsevier Science B.V. All rights reserved.

Keywords: Bivalent metals; 4-Methylbenzylidenepyruvate; Coordination sites; Thermal behaviour

1. Introduction

Synthesis of benzylidenepyruvic acid (HBP), as well as of phenyl-substituted derivatives of HBP, have been reported [1,2]. These acids are of continuing interest as intermediates in pharmacological, industrial and chemical syntheses, in the development of enzyme inhibitors and drugs, as model substrates of enzymes, and in other ways [2–7].

Preparation and investigation of several metal-ion complexes of phenyl-substituted derivatives of BP, have been carried out in aqueous solutions [8–11], and in the solid state [12–18]. In aqueous solutions, these works reported mainly the thermodynamic stability (β_1) and spectroscopic parameters ($\epsilon_{1\max}$,

λ_{\max}), associated with 1:1 complex species, analytical applications of the ligands, e.g., in gravimetric analysis and as metallochromic indicators, while in the solid state, the establishment of the stoichiometry and detailed knowledge of the thermal behaviour of the ligands and their metal-ion compounds have been the main purposes of these studies.

In the present paper, solid state compounds of bivalent manganese, iron, cobalt, nickel, copper, zinc and lead with 4-methylbenzylidenepyruvate (4-CH₃-C₆H₄-CH=CH-COCOO⁻) were prepared. The compounds were investigated by complexometry, elemental analysis, X-ray powder diffractometry, infrared spectroscopy, simultaneous thermogravimetry-differential thermal analysis (TG-DTA) and differential scanning calorimetry (DSC). The data provide information concerning the thermal stability and thermal decomposition of these compounds in the solid state.

* Corresponding author. Tel.: +55-16201-6617;

fax: +55-16222-7932.

E-mail address: massaio@iq.unesp.br (M. Ionashiro).

2. Experimental

The sodium salt of 4-methylbenzylidenepyruvic acid (4-Me-BP) was prepared from 4-methylbenzaldehyde and sodium pyruvate in the presence of an alkaline catalyst as described in the literature [19]. Aqueous solutions of the bivalent metal ions were prepared by dissolving the corresponding chlorides, except for lead, where the nitrate was used.

The solid state compounds were prepared by adding slowly, with continuous stirring, the ligand solution to the respective metal-ion solutions until complete precipitation of the metal ions. To avoid oxidation of Mn(II) and Fe(II), all their solutions as well as the water employed for washing their precipitates were purged with nitrogen gas.

The precipitates were washed until chloride (or nitrate) ions were eliminated, filtered through and dried on Whatman no. 42 filter paper and kept in a desiccator over anhydrous calcium chloride, under reduced pressure (10^3 Pa), to constant mass.

In the solid state compounds, metal ions, water and 4-Me-BP contents were determined from the TG curves. The metal ions were also determined by complexometry with standard EDTA solution [20,21] after igniting the compounds to the respective oxides and their dissolution in hydrochloric or nitric acid.

Simultaneous TG-DTA and DSC curves were obtained with two thermal analysis systems, models SDT 2960 and DSC 2010, both from TA Instruments. The purge gas was an air flow of 150 ml min^{-1} . A heating rate of $10^\circ\text{C min}^{-1}$ was adopted, with samples weighing about 7–8 mg. Alumina and aluminium crucibles, the latter with perforated covers, were used for TG-DTA and DSC, respectively.

Carbon and hydrogen contents were determined by microanalytical procedures, with an EA1110 CHNS-0 Elemental Analyser from CE Instruments.

Table 1

Analytical data for the $\text{ML}_2 \cdot n\text{H}_2\text{O}$ compounds^a

	M (%)			L (lost) (%)		H ₂ O (%)		C (%)		H (%)		Final residue
	Calcd.	EDTA	TG	Calcd.	TG	Calcd.	TG	Calcd.	EA	Calcd.	EA	
MnL ₂ ·2H ₂ O	11.70	11.35	11.81	76.05	75.93	7.68	7.70	56.29	56.52	4.73	4.65	Mn ₃ O ₄
FeL ₂ ·2H ₂ O	11.88	11.54	11.90	75.36	75.18	7.66	7.59	56.18	56.67	4.72	4.66	Fe ₂ O ₃
CoL ₂ ·2H ₂ O	12.45	11.93	12.34	76.56	76.74	7.61	7.63	55.82	55.86	4.69	4.72	CoO
NiL ₂ ·3H ₂ O	11.95	11.95	12.02	73.78	73.80	11.01	10.90	53.79	53.41	4.94	4.16	NiO
CuL ₂ ·2H ₂ O	13.30	13.70	13.61	75.82	75.90	7.54	7.41	55.28	56.03	4.65	4.33	CuO
ZnL ₂ ·3H ₂ O	13.13	12.96	13.10	72.80	72.90	10.86	10.80	53.07	52.59	4.87	4.46	ZnO
PbL ₂	34.38	35.35	35.30	61.89	61.95	–	–	45.12	45.06	3.10	3.26	PbO

^a M: metal; L: 4-methylbenzylidenepyruvate.

Table 2

Spectroscopic data for sodium 4-methylbenzylidenepyruvate (4-Me-BP) and compounds with some bivalent metal ions^a

Compound	$\nu_{\text{as}}(\text{COO}^-)^{\text{b}}$ (cm^{-1})	$\Delta\nu_{\text{as}}(\text{COO}^-)^{\text{c}}$	$\nu_{\text{sym}}(\text{COO}^-)$ (cm^{-1}) ^b	$\nu(\text{C=O})^{\text{d}}$ (cm^{-1})	$\Delta\nu(\text{C=O})^{\text{e}}$
4Me-BP-Na·0.5H ₂ O	1635s; 1605s	–	1411m	1673m	–
Mn(4Me-BP) ₂ ·2H ₂ O	1635s; 1601s	0; 4	1413m	1673sh	0
Fe(4Me-BP) ₂ ·2H ₂ O	1635s; 1594s	0; 11	1407m	1667sh	6
Co(4Me-BP) ₂ ·2H ₂ O	1635s; 1590s	0; 15	1407m	1664sh	9
Ni(4Me-BP) ₂ ·3H ₂ O	1585s; 1563s	50; 42	1400m	1645s	28
Cu(4Me-BP) ₂ ·2H ₂ O	1564s	71	1384m	1623m	50
Zn(4Me-BP) ₂ ·3H ₂ O	1589s; 1563s	46; 42	1409m	1631sh	42
Pb(4Me-BP) ₂	1598s; 1562s	37; 43	1397m	1626sh	47

^a s: strong, m: medium, sh: shoulder.

^b $\nu_{\text{sym}}(\text{COO}^-)$ and $\nu_{\text{as}}(\text{COO}^-)$: symmetrical and anti-symmetrical vibrations of the COO^- group, respectively.

^c $\nu_{\text{as}}(\text{COO}^-)$ (Na salt) – $\nu_{\text{as}}(\text{COO}^-)$ (metal complex).

^d Ketonic carbonyl stretching frequency.

^e $\nu(\text{C=O})$ (Na salt) – $\nu(\text{C=O})$ (metal complex).

X-ray powder patterns were obtained with a Siemens D-500 X-ray diffractometer using Cu K α radiation ($\lambda = 1.544 \text{ \AA}$) and settings of 40 kV and 20 mA.

Infrared spectra for 4-Me-BP (sodium salt) as well as for its metal-ion compounds, were run on a Nicolet model Impact 400 FT-IR instrument, within the 4000–400 cm^{-1} range. The solid samples were pressed into KBr pellets.

3. Results and discussion

The analytical and thermoanalytical (TG) data are shown in Table 1. These results establish the stoichiometry of these compounds, which are in agreement with the general formula: $M(4\text{-Me-BP})_2 \cdot n\text{H}_2\text{O}$, where M represents Mn(II), Fe(II), Co(II), Ni(II), Cu(II), Zn(II) or Pb(II), 4-Me-BP is 4-methylbenzylidenepyruvate and $n = 0, 2$ or 3.

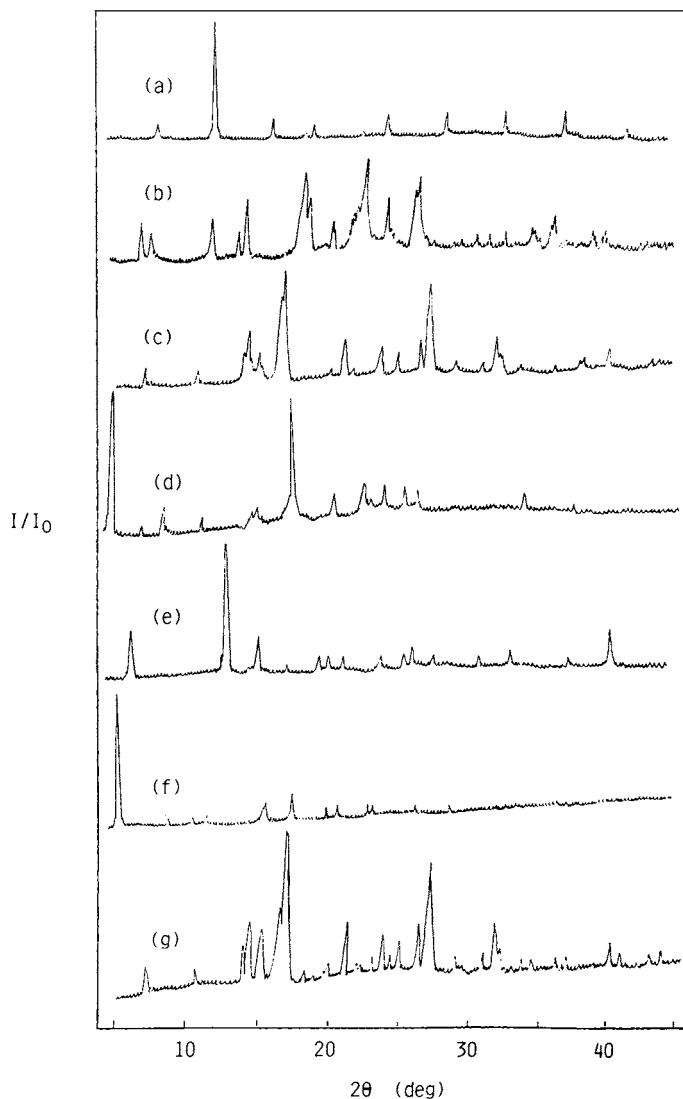


Fig. 1. X-ray powder diffraction patterns of (a) $\text{Mn}(4\text{-Me-BP})_2 \cdot 2\text{H}_2\text{O}$, (b) $\text{Fe}(4\text{-Me-BP})_2 \cdot 2\text{H}_2\text{O}$, (c) $\text{Co}(4\text{-Me-BP})_2 \cdot 2\text{H}_2\text{O}$, (d) $\text{Ni}(4\text{-Me-BP})_2 \cdot 3\text{H}_2\text{O}$, (e) $\text{Cu}(4\text{-Me-BP})_2 \cdot 2\text{H}_2\text{O}$, (f) $\text{Zn}(4\text{-Me-BP})_2 \cdot 3\text{H}_2\text{O}$ and (g) $\text{Pb}(4\text{-Me-BP})_2$.

The X-ray diffraction powder patterns (Fig. 1) show that all the compounds have a crystalline structure, without evidence of the formation of isomorphous series.

Infrared spectroscopic data on 4-methylbenzylidene-pyruvate and its compounds with the metal ions considered in this work are shown in Table 2. The investigation was focused mainly within the 1700–1400 cm^{-1} range because this region is potentially

most informative in attempting to assign coordination sites.

In 4-Me-BP (sodium salt), strong doublet bands (at 1635 and 1605 cm^{-1}) and a medium intensity band located at 1411 cm^{-1} are attributed to the anti-symmetrical and symmetrical frequencies of the carboxylate groups, respectively [22,23]. The band centered at 1673 cm^{-1} is typical of a conjugated ketonic carbonyl group [22–24]. This is in line with the

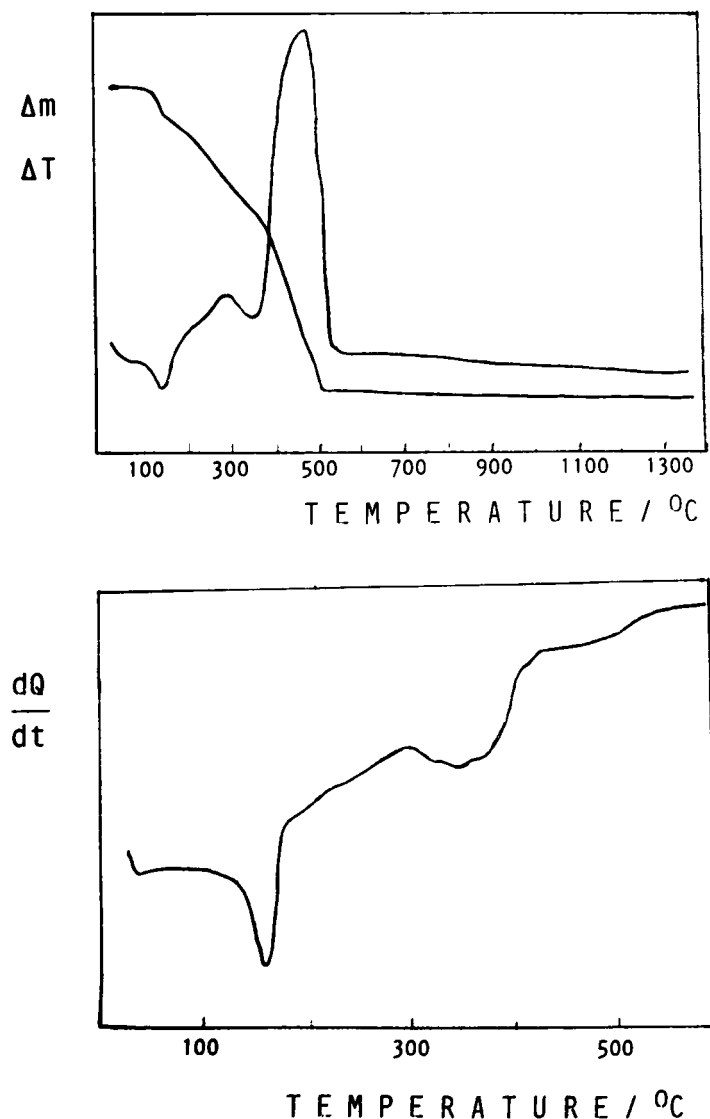


Fig. 2. TG-DTA and DSC curves of $\text{Mn}(4\text{-Me-BP})_2 \cdot 2\text{H}_2\text{O}$ ($m = 7.191$ and 6.521 mg, respectively).

observed carbonyl stretching frequency for *s-trans*-benzylidene acetone (i.e., 1674 cm^{-1}) [23].

Except for the Cu(II) compound, the doublet bands assigned to the anti-symmetrical stretching carboxylate frequencies are retained in the complexes. Both these bands as well as that assigned to the ketonic carbonyl are shifted to lower values relative to the corresponding frequencies in 4-Me-BP itself (sodium salt). This behaviour indicates that both groups act as

coordination centres in the metal compounds [24,25]. The data displayed in Table 2 show that these shifts are dependent on the metal ions and the magnitudes of the shifts follow the well-known Irving–Williams order: $\text{Mn(II)} < \text{Fe(II)} < \text{Co(II)} < \text{Ni(II)} < \text{Cu(II)} > \text{Zn(II)}$. Overall, the information conveyed by the infrared spectra is in line with that gathered for the 1:1 complexes of the same ligand with several metal ions in aqueous solution, where linear free energy

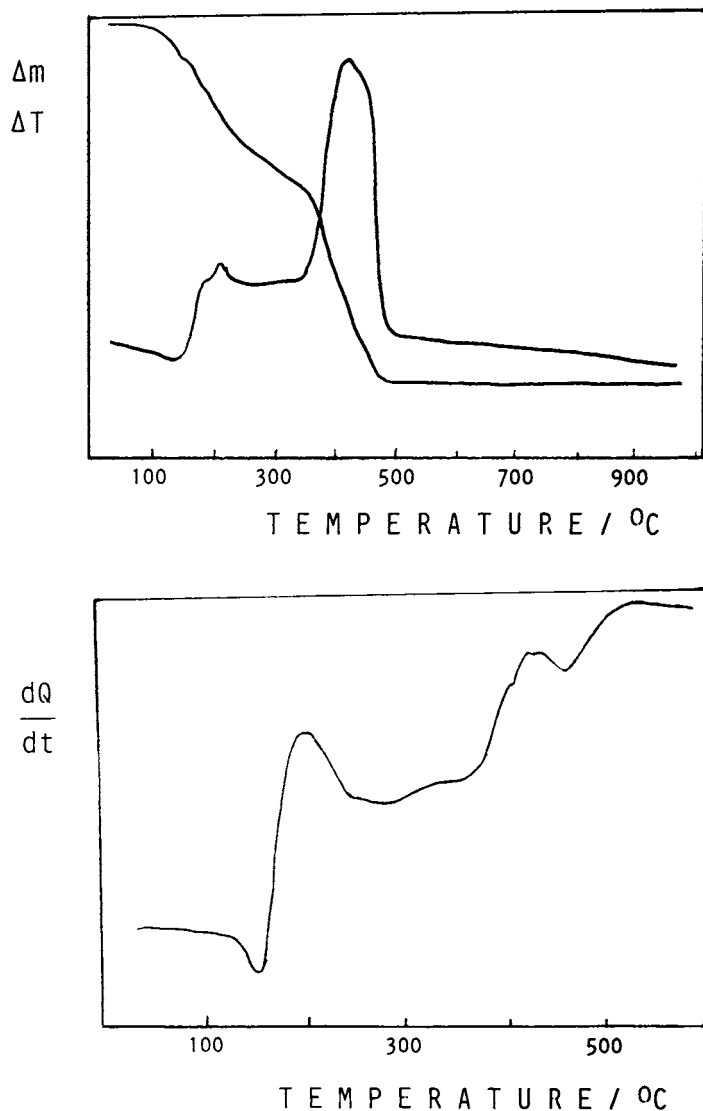


Fig. 3. TG-DTA and DSC curves of $\text{Fe(4-Me-BP)}_2 \cdot 2\text{H}_2\text{O}$ ($m = 7.643$ and 7.604 mg, respectively).

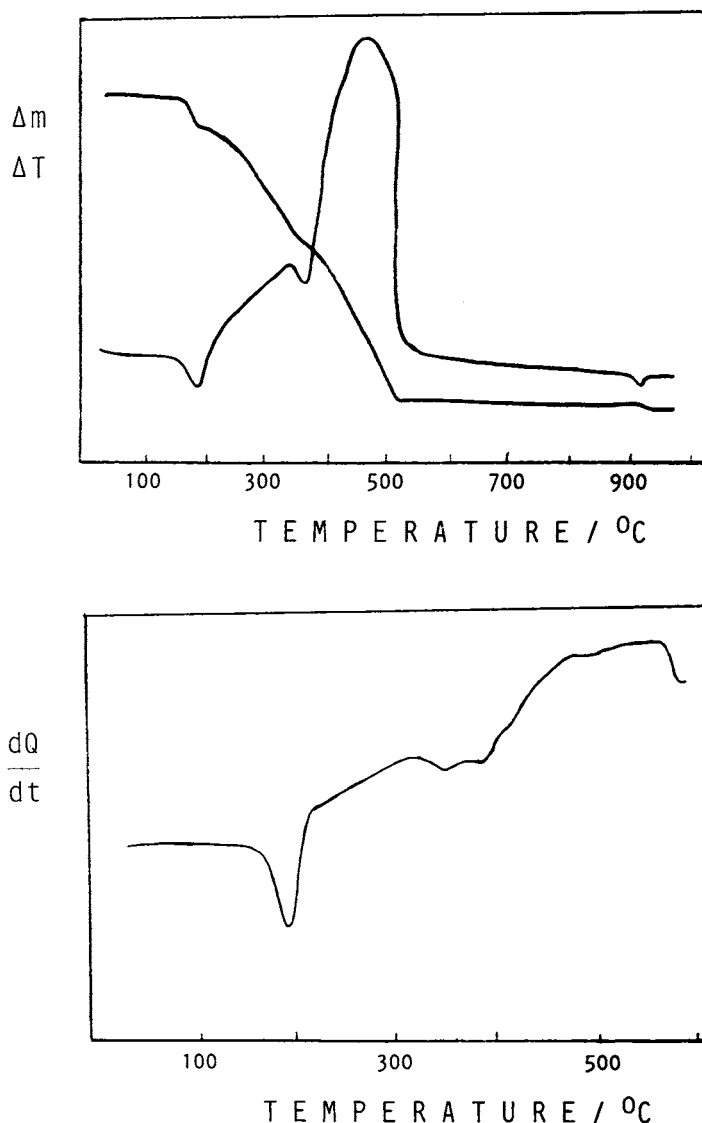


Fig. 4. TG-DTA and DSC curves of $\text{Co}(4\text{-Me-BP})_2 \cdot 2\text{H}_2\text{O}$ ($m = 7.638$ and 7.899 mg, respectively).

relationships, also suggest the $-\text{COCOO}^-$ moiety as the bidentate metal binding site of 4-Me-BP [11].

Simultaneous TG-DTA and DSC curves of the compounds are shown in Figs. 2–8. The TG-DTA curves show mass losses in three, four or six steps, corresponding to endothermic peaks due to dehydration and exothermic peaks attributed to the oxidation of organic matter. The DSC curves, also show endothermic and exothermic peaks, corresponding to the mass

losses displayed by the TG curves. Small differences observed concerning the peak temperatures obtained by TG-DTA and DSC for the endothermic peaks are undoubtedly due to the perforated cover used to obtain the DSC curves, while the TG-DTA ones are obtained without cover.

The thermal stability of the anhydrous compounds (I), as well as the final temperature of thermal decomposition (II) as shown by the TG-DTA curves, depend

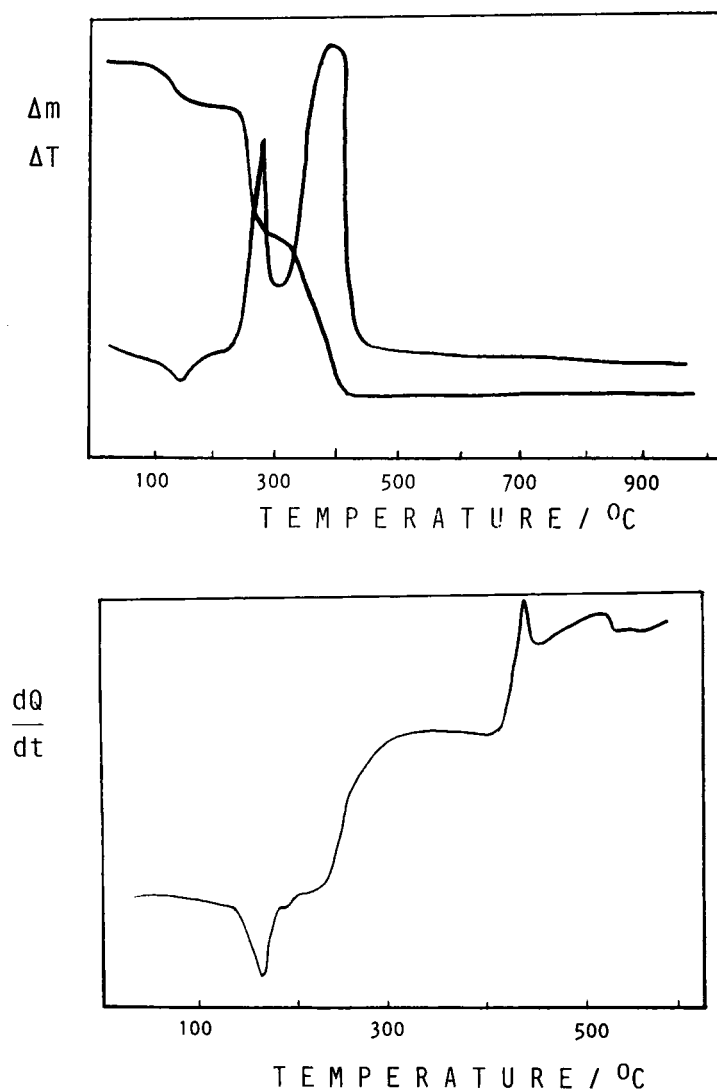


Fig. 5. TG-DTA and DSC curves of $\text{Ni}(\text{4-Me-BP})_2 \cdot 3\text{H}_2\text{O}$ ($m = 7.807$ and 3.906 mg, respectively).

on the nature of the metal ion, and they follow the order:

(I) $\text{Ni} > \text{Zn} > \text{Co} > \text{Pb} > \text{Cu} > \text{Mn} \approx \text{Fe}$

(II) $\text{Zn} > \text{Pb} > \text{Cu} > \text{Mn} \approx \text{Co} > \text{Fe} > \text{Ni}$

The thermal behaviour of the compounds is heavily dependent on the nature of the metal ion and so the features of each of these compounds are discussed individually below.

- *Manganese compound.* The simultaneous TG-DTA curves and the DSC curve as well are shown in Fig. 2. The first mass loss observed between 100 and 150°C (TG), corresponding to an endothermic peak at 150°C (DTA) and 160°C (DSC) is due to hydration water; it reflects the loss of $2\text{H}_2\text{O}$ (calcd. = 7.68%, TG = 7.70%). The thermal decomposition of the anhydrous compound occurs in two overlapping steps: between 150 and 380, and 380 and 520°C, with losses of 30.54 and 45.39%,

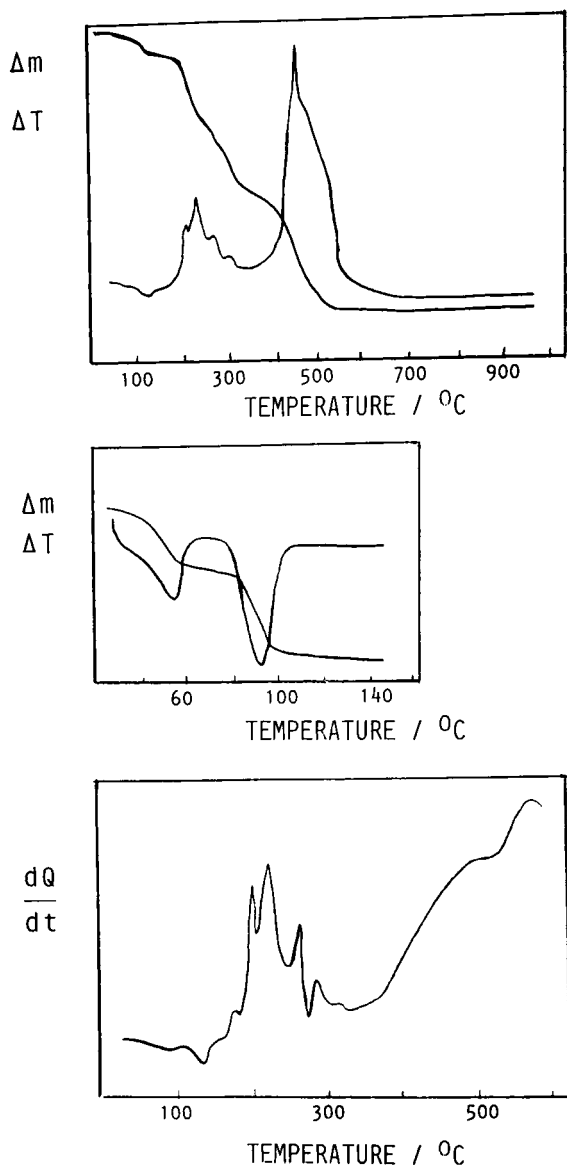


Fig. 6. TG-DTA and DSC curves of $\text{Cu}(4\text{-Me-BP})_2 \cdot 2\text{H}_2\text{O}$ ($m = 7.585$ and 3.906 mg, respectively).

respectively, corresponding to the exothermic peaks at 300 and 460°C (DTA) or the broad exotherms between 200 and $>600^\circ\text{C}$ (DSC), which are attributed to oxidation of the organic matter. The total mass loss up to 520°C is in agreement with the formation of Mn_2O_3 (calcd. = 83.76% , TG = 83.61%). The last mass loss observed between 920 and 980°C , corresponding to the small endothermic

peak at 950°C (DTA), is assigned to the reduction of Mn_2O_3 to Mn_3O_4 (calcd. = 0.57% , TG = 0.63%) and confirmed by X-ray powder diffractometry.

Literature reports on the thermal stability and reduction temperature of Mn_2O_3 are in disagreement among themselves [26–28] and with the data obtained in this work. This behaviour concerning manganese oxides has already been pointed out [26]; it is reported that the properties significantly depend on the preparation conditions, structural properties of the oxides and upon operational parameters during the reduction step [26].

- *Iron compound.* The simultaneous TG-DTA and DSC curves are shown in Fig. 3. The first mass loss observed between 80 and 150°C (TG), corresponding to endothermic peak at 150°C (DTA) and 155°C (DSC) is due to dehydration with loss of $2\text{H}_2\text{O}$ (calcd. = 7.66% , TG = 7.59%). Immediately after the dehydration, the anhydrous compounds show mass losses in three overlapping steps: between 150 and 180°C (6.27%), 180 and 350°C (24.36%), and 350 and 480°C (44.55%), corresponding to the exothermic peaks at 210 and 415°C (DTA) and 200 , 420 and 530°C (DSC), attributed to oxidation of Fe(II) to Fe(III) and of the organic matter. The total mass loss up to 480°C is in agreement with the formation of Fe_2O_3 as the final residue (calcd. = 83.02% , TG = 82.77%) which was confirmed by X-ray powder diffractometry.
- *Cobalt compound.* The simultaneous TG-DTA and DSC curves are shown in Fig. 4. The first mass loss that occurs between 120 and 185°C (TG), corresponding to endothermic peak at 180°C (DTA) or 190°C (DSC), is due to dehydration with loss of $2\text{H}_2\text{O}$ (calcd. = 7.61% , TG = 7.63%). The thermal decomposition of the anhydrous compound occurs in two overlapping steps: between 190 and 350 , and 350 and 520°C , with losses of 30.45 and 45.07% , respectively, corresponding to exothermic peaks at 340 and 470°C (DTA) or the broad exotherms between 220 and 600°C , attributed to the oxidation of the organic matter. The total mass loss up to 520°C is in agreement with the formation of Co_3O_4 (calcd. = 83.04% , TG = 83.15%). The last mass loss that occurs between 900 and 930°C , corresponding to the endothermic peak at 920°C (DTA), is attributed to reduction of Co_3O_4 to CoO (calcd. = 1.18% , TG = 1.22%), in agreement with

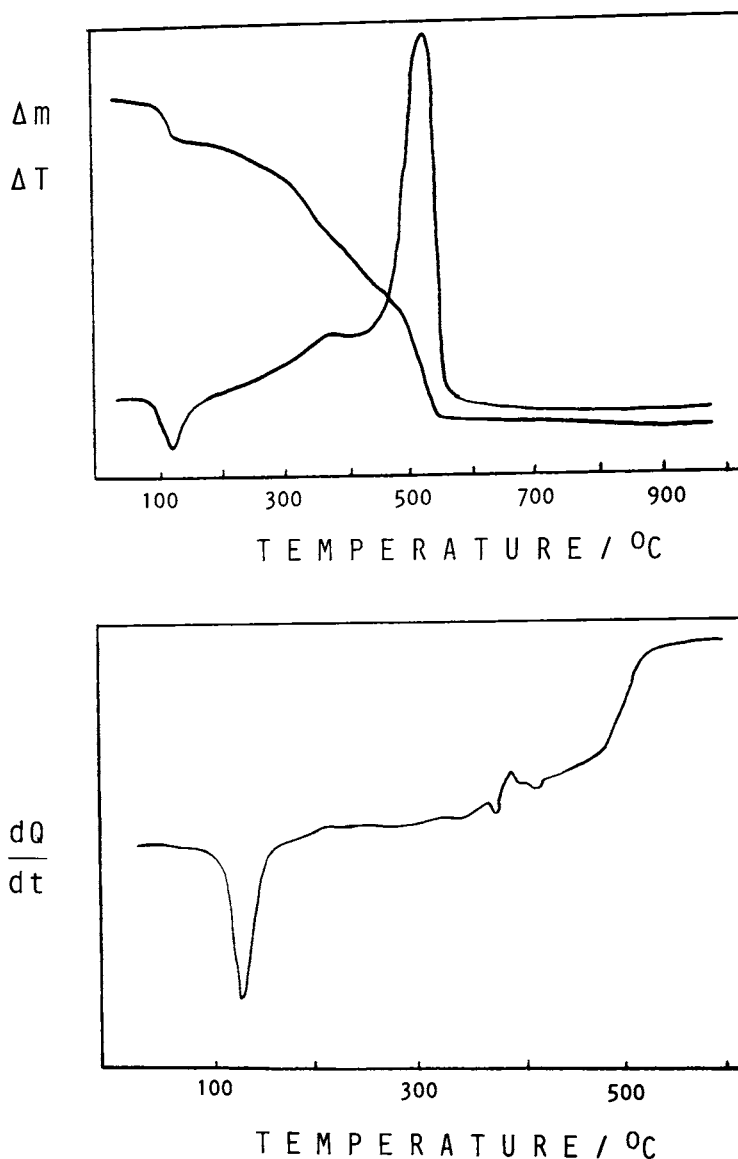


Fig. 7. TG-DTA and DSC curves of $\text{Zn(4-Me-BP)}_2 \cdot 3\text{H}_2\text{O}$ ($m = 7.159$ and 5.626 mg, respectively).

the literature [29,30]. The X-ray powder pattern of the residue obtained at 950°C , is coincident with that obtained for Co_3O_4 , this is due to the reoxidation reaction of CoO to Co_3O_4 which occurs on cooling the former in an air atmosphere at room temperature [29,30].

- *Nickel compound.* The TG-DTA and DSC curves are shown in Fig. 5. The mass loss that occurs between

70 and 170°C (TG), corresponding to endothermic peak at 150°C (DTA) or 165°C (DSC), is due to dehydration with loss of $3\text{H}_2\text{O}$ (calcd. = 11.01% , TG = 10.90%). The anhydrous compound is stable up to 220°C , and above this temperature the thermal decomposition occurs in two consecutive steps: between 220 and 295 , and 295 and 425°C with losses of 29.45 and 44.35% , respectively. These

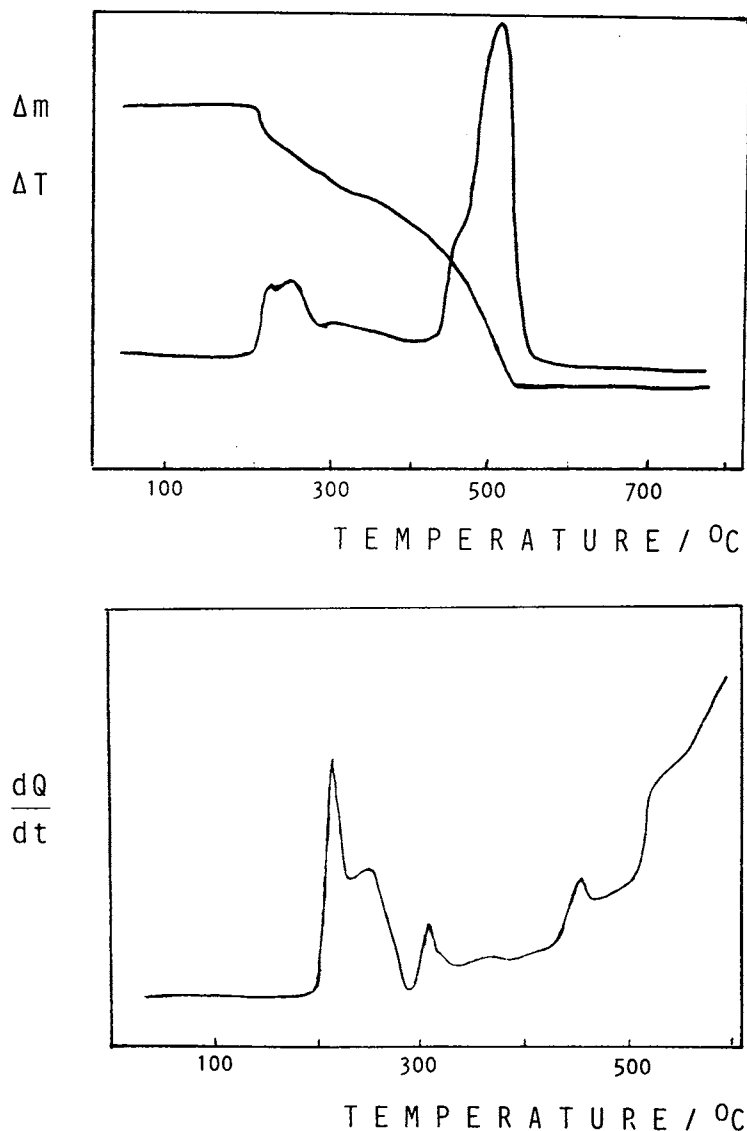


Fig. 8. TG-DTA and DSC curves of $\text{Pb}(4\text{-Me-BP})_2$ ($m = 7.141$ and 7.102 mg, respectively).

mass losses correspond to exothermic peaks at 280 and 400 °C (DTA) or the broad exotherms between 220 and >600 °C (DSC), attributed to oxidation of the organic matter. The total mass loss up to 425 °C, is in agreement with the formation of NiO as final residue (calcd. = 84.79%, TG = 84.70%), and confirmed by X-ray powder diffractometry.

- *Copper compound.* The TG-DTA and DSC curves are shown in Fig. 6. The mass loss observed up

to 130 °C (TG), with evidence of two consecutive steps, corresponding to an endothermic peak at 120 °C (DTA) (Fig. 6), or 100 and 130 °C (DSC), is due to dehydration with loss of $2\text{H}_2\text{O}$ (calcd. = 7.54%, TG = 7.41%). Aiming at a closer examination of the dehydration process, TG-DTA curves were obtained up to 150 °C in static air atmosphere, sample mass: 5.387 mg, and heating rate of 2°C min^{-1} (Fig. 6). These curves confirmed

that the dehydration occurs in two steps: between 30 and 60, and 75 and 100 °C, corresponding to endothermic peaks at 55 and 95 °C; dehydration in two steps is also pointed out by the DSC curve.

The anhydrous compound is stable up to 170 °C, and above this temperature the thermal decomposition occurs in four consecutive and/or overlapping steps with losses of 9.02% (170–220 °C), 8.97% (220–240 °C), 21.31% (240–320 °C) and 36.60% (320–530 °C). These mass losses correspond to exothermic peaks at 190, 220, 260 and 430 °C (DTA), although the DSC curve shows five exothermic peaks (160–320 °C) and a large exotherm between 320 and 600 °C. The total mass loss up to 530 °C is in agreement with the formation of CuO as the final residue (calcd. = 83.36%, TG = 83.31%), which was confirmed by X-ray powder diffractometry.

- **Zinc compound.** The TG-DTA and DSC curves are shown in Fig. 7. The mass loss observed between 70 and 130 °C (TG), corresponding to the endothermic peak at 120 °C (DTA) or 130 °C (DSC), is due to hydration water with loss of 3H₂O (calcd. = 10.86%, TG = 10.80%). The anhydrous compound is stable up to 195 °C, and above this temperature the thermal decomposition occurs in two overlapping steps with mass losses of 28.84% (195–395 °C) and 44.06% (395–550 °C), corresponding to exothermic peaks at 380 and 460 °C (DTA) or the exotherms between 300 and >600 °C (DSC), attributed to oxidation of organic matter. The total mass loss up to 550 °C is in agreement with the formation of ZnO, as the final residue (calcd. = 83.66%, TG = 83.70%); this was confirmed by X-ray powder diffractometry.
- **Lead compound.** The TG-DTA and DSC curves are shown in Fig. 8. These curves show that this compound was obtained in the anhydrous state and it is stable up to 180 °C. Above this temperature up to 535 °C, the TG-DTA curves suggest mass losses in four overlapping steps, while the DSC curve suggests five steps. The mass loss that occurs between 180 and 305 °C (18.28%), and 305 and 535 °C (43.67%), corresponding to exothermic peaks at 220, 250, 300 and 510 °C (DTA) or 200, 250, 305, 460 and >600 °C (DSC), are attributed to oxidation of the organic matter. The total mass loss up to 535 °C, is in agreement with the formation of PbO, as the final residue (calcd. = 61.89%,

TG = 61.95%); this was further confirmed by X-ray powder diffractometry.

4. Conclusion

From TG, complexometry and elemental analysis data, a general formula could be established for the binary compounds involving some bivalent metal ions and 4-Me-BP. The X-ray powder patterns pointed out that the synthesized compounds have a crystalline structure, without evidence concerning the formation of isomorphous series. The infrared spectroscopic data suggest that 4-Me-BP acts as a bidentate ligand towards the metal ions considered in this work.

The TG-DTA and DSC curves, provided previously unreported information about the thermal stability and thermal decomposition of these compounds.

Acknowledgements

The authors thank FAPESP (Procs. 97/12646-8 and 98/12794-0) and CNPq Foundations (Brazil) for financial support and Ms. Rosemary Camargo for aid in the preparation of this manuscript.

References

- [1] E.D. Stecher, M.J. Incorvia, B. Kerben, D. Lavine, M. Oen, E. Suhl, *J. Org. Chem.* 38 (1973) 4453 and references cited therein.
- [2] A.J.L. Cooper, J.Z. Ginos, A. Meister, *Chem. Rev.* 83 (1983) 321.
- [3] A.K. Datta, T.C. Daniels, *J. Pharm. Sci.* 52 (1963) 905.
- [4] W. Mayer, H. Rudolph, E. de Cleur, *Angew. Makromol. Chem.* 93 (1981) 83.
- [5] A.I. Baba, W. Wang, W.Y. Kim, L. Strong, R.H. Schmehl, *Synth. Commun.* 24 (1994) 1029.
- [6] G. Dujardin, M. Maudet, E. Brown, *Tetrahedron Lett.* 38 (1997) 1555.
- [7] G. Dujardin, S. Leconte, A. Bernard, E. Brown, *Synlett* (2001) 147 and references cited therein 1 (2001) 147.
- [8] C.B. Melios, V.R. Torres, M.H.A. Mota, J.O. Tognolli, M. Molina, *Analyst* 109 (1984) 385.
- [9] C.B. Melios, J.T.S. Campos, M.A.C. Mazzeu, L.L. Campos, M. Molina, J.O. Tognolli, *Inorg. Chim. Acta* 139 (1987) 163.
- [10] C.B. Melios, M. Ionashiro, H. Redigolo, M.H. Miyano, M. Molina, *Eur. J. Solid State Inorg. Chem.* 28 (1991) 291.
- [11] R.N. Marques, C.B. Melios, N.C.S. Pereira, O.S. Siqueira, M. de Moraes, M. Molina, M. Ionashiro, *J. Alloys Comp.* 249 (1997) 102.

- [12] L.C.S. Oliveira, C.B. Melios, C.A. Ribeiro, M.S. Crespi, M. Ionashiro, *Thermochim. Acta* 219 (1993) 215.
- [13] M.H. Miyano, C.B. Melios, C.A. Ribeiro, H. Redigolo, M. Ionashiro, *Thermochim. Acta* 221 (1993) 53.
- [14] D.E. Raseira, L.S.C. Oliveira, C.B. Melios, M. Ionashiro, *Thermochim. Acta* 250 (1995) 151.
- [15] L.C.S. Oliveira, D.E. Raseira, O.S. Siqueira, J.R. Matos, C.B. Melios, M. Ionashiro, *Thermochim. Acta* 275 (1996) 269.
- [16] L.C.S. Oliveira, D.E. Raseira, J.D.S. Oliveira, C.B. Melios, M. Ionashiro, *Ann. Assoc. Bras. Quim.* 47 (1988) 75.
- [17] R.A. Mendes, M.A.S. Carvalho Filho, N.S. Fernandes, L.M. D'Assunção, C.B. Melios, M. Ionashiro, *Ann. Assoc. Bras. Quim.* 47 (1998) 329.
- [18] N.S. Fernandes, M.A.S. Carvalho Filho, C.B. Melios, M. Ionashiro, *J. Therm. Anal. Cal.* 59 (2000) 663.
- [19] C. Melios, A.M. Delsin, J.O. Tognolli, M. Molina, *Ecl. Quim.* 6 (1981) 51.
- [20] H.A. Flaschka, *EDTA Titrations*, Pergamon Press, Oxford, 1964.
- [21] C.N. de Oliveira, M. Ionashiro, C.A.F. Graner, *Ecl. Quim.* 10 (1985) 7.
- [22] G. Socrates, *Infrared Characteristic Group Frequencies*, 2nd ed., Wiley, New York, 1994, pp. 91 and 236–237.
- [23] R.M. Silverstein, F.X. Webster, *Spectrometric Identification of Organic Compounds*, 6th ed., Wiley, New York, 1998, pp. 92, 93, 96 and 97.
- [24] F.A. Cotton, in: J. Lewis, R.G. Wilkins (Eds.), *The Infrared Spectra of Transition Metal Complexes in Modern Coordination Chemistry*, Interscience, New York, 1960, pp. 379–386.
- [25] K. Nakamoto, *Infrared and Raman Spectra of Inorganic and Coordination Compounds, Part B*, 5th ed., Wiley, New York, 1997, pp. 58–61.
- [26] C. Gonzales, J.I. Gutierrez, J.R. Gonzalez-Velasco, A. Cid, A. Arranz, J.F. Arranz, *J. Therm. Anal.* 47 (1996) 93.
- [27] D. Czakis-Sulikowska, J. Katuzna, *J. Therm. Anal. Cal.* 58 (1999) 51.
- [28] L. Biernacki, S. Pokrzywnicki, *J. Therm. Anal. Cal.* 55 (1999) 227.
- [29] G.A. El-Shobaky, A.S. Ahmad, A.N. Al Noaimi, H.G. El-Shobaky, *J. Therm. Anal.* 46 (1996) 1801.
- [30] Z.P. Xu, H.C. Zeng, *J. Mater. Chem.* 8 (1998) 2499.